

Chandra DETECTION OF AN X-RAY FLARE FROM THE BROWN DWARF LP 944-20

ROBERT E. RUTLEDGE

Division of Physics, Mathematics and Astronomy
MS 220-47, California Institute of Technology, Pasadena, CA 91107
rutledge@srl.caltech.edu

GIBOR BASRI

Department of Astronomy, University of California at Berkeley
Berkeley, CA 94720-3411
basri@soleil.berkeley.edu
EDUARDO L. MARTÍN

Division of Geological and Planetary Sciences, California Institute of Technology
MS 150-21, Pasadena, CA 91125
ege@gps.caltech.edu

AND

LARS BILDSTEN

Institute for Theoretical Physics and Department of Physics
Kohn Hall, University of California, Santa Barbara, CA 93106
bildsten@itp.ucsb.edu

ApJ Letters, Submitted April 28, 2000; Revised May 17, 2000

ABSTRACT

We have detected a bright X-ray flare from the nearby ($d=5.0$ pc) brown dwarf LP 944-20 with the *Chandra*/ACIS-S. This is an old (500 Myr), rapidly rotating, lithium-bearing M9 object, with a bolometric luminosity of $\approx 6 \times 10^{29}$ erg sec⁻¹. It was only detected by *Chandra* during an X-ray flare of duration 1-2 hours near the end of a 12.1 hour observation. The peak X-ray luminosity was $1.2_{-0.3}^{+0.5} \times 10^{26}$ erg sec⁻¹ in the brightest ≈ 550 seconds, corresponding to $L_X/L_{\text{bol}} \approx 2 \times 10^{-4}$. A total of 2×10^{29} ergs was released during the 43,773 sec observation, giving a time-averaged $L_X/L_{\text{bol}} \approx 7 \times 10^{-6}$. LP 944-20 was not detected before the flare, with a 3σ upper limit on the emission at $L_X/L_{\text{bol}} < 2 \times 10^{-6}$ ($L_X < 1 \times 10^{24}$ erg sec⁻¹). This is faint for a rapidly rotating late-type star, and establishes a record lower limit to the quiescent flux about an order of magnitude below the flux limit (and a factor of 5 below the L_X/L_{bol} limit) placed on quiescent X-ray emission from the M8 dwarf VB 10. The inferred flaring duty cycle is comparable to that measured via variable H α emission for other late M-type, fully convective stars.

Subject headings: stars: coroneae – stars: low-mass, brown dwarfs – stars: individual(LP 944-20)

1. INTRODUCTION

LP 944-20 (=BRI 0337–3535) is an isolated, non-accreting, brown dwarf identified through its Li abundance and low luminosity (Tinney 1998). Its parallactic distance and bolometric luminosity are 5.0 ± 0.1 pc and 6×10^{29} erg sec⁻¹ (Tinney 1996). Tinney (1998) infers an age of about $\tau = 500$ Myr, which implies that it is a fully collapsed object (see Feigelson & Montmerle 1999 for a recent review of protostellar evolution). This requires that any observed coronal activity not be due to accretion, as may power younger brown dwarfs ($\tau < 10$ Myr) in analogy with T-Tauri stars. We report here on a bright 1-2 hour X-ray flare detected with *Chandra* during a 12 hour observation, and a strong upper limit on persistent X-ray emission. We attribute the energy release in the flare to transient magnetic activity on this fully convective, rapidly rotating star.

Stars with masses $M > 0.3M_{\odot}$ have an outer convective zone and an interior radiative region that need not be rotating at the same rate. A poloidal magnetic field in the convective layers will be stretched and amplified into strong toroidal fields when it is dragged by convective overshoot (see Weiss 1996) into the radial shear in rotation that resides at the boundary (in and near the so-called "tachocline"; Spiegel & Zahn 1992). In these cases, rapid rotation is associated with enhanced coronal activity. The activity level correlates with the Rossby number – the ratio of the stellar rotation period to the convective turnover time (Noyes et al. 1984). For Rossby numbers between 10 and

0.1, coronal activity (as measured by L_X/L_{bol}) increases with decreasing Rossby number (that is, with more rapid rotation), "saturating" at about $L_X/L_{\text{bol}} \sim 10^{-3}$ for Rossby numbers of 0.1 to 0.01 (Randich 1997).

For less massive stars and young brown dwarfs, the energy is transported throughout the star by convection; no radiative core is present. For this reason, it has been supposed that the activity and its dependence on rotation might change near the spectral type where the radiative layer disappears (about M5.5; see Giampapa et al. 1996 for a physical overview). However, a search for this effect found no evidence for a change in the saturated value of $L_X/L_{\text{bol}} \sim 10^{-3}$, down to spectral types as late as M7, well into the region of fully convective stars (Fleming et al. 1993). This implied no dramatic change in the rotation-activity dependence in fully convective stars.

The first hint that activity might be decreasing in the very late M dwarfs was observed from the rapidly rotating ($v \sin i = 40$ km sec⁻¹) M9.5 star BRI 0021-0214, for which a strong upper-limit on H α emission indicated a substantially lower persistent coronal activity than expected from a rapidly rotating, fully convective star (Basri & Marcy 1995). On the other hand, Reid et al. (1999) observed a strong H α flare from BRI 0021-0214; this indicated that activity was indeed present, and that the star has outbursts no more than 7% of the time. Liebert et al. (1999) reported a bright H α flare from 2MASSW J0149090+295613, an M9.5 V star which is otherwise quiescent. Intensity variabil-

ity from brown dwarfs has been searched for, with limited success. Bailer-Jones & Mundt (1999) found no infra-red variability in three Pleiades brown dwarfs, with a limit of $\delta I < 0.05$ mag on timescales between 25 min–27 hrs. A search for “weather” in two brown dwarfs (LP 944-20 and DENIS-P J1228-1547) produced a claim of evidence of variability in one, at the 2.3σ level (Tinney & Tolley 1999).

Previous X-ray observations of brown dwarfs and brown dwarf candidates have produced detections of persistent emission from several (Neuhäuser & Comerón 1998; Neuhäuser et al. 1999), but these are all young objects ($\lesssim 10$ My), still in the process of proto-stellar collapse, and so are actively accreting; neither are they as cool or faint as older brown dwarfs such as LP 944-20. The activity observed from these collapsing brown dwarfs is analogous to that in the also-young T-Tauri stars – powered by accretion and collapse – rather than that in fully collapsed, older M dwarfs. There are only a few observations of X-ray emission in older late M dwarfs and brown dwarfs. Giampapa et al. (1996) reported on a ROSAT detection from VB 8 (spectral type M7) with a time-averaged $L_X/L_{\text{bol}}=1.6 \times 10^{-3}$. Fleming et al. (2000) detected the M8 star VB 10 during a flare at $L_X/L_{\text{bol}}=5 \times 10^{-4}$. No quiescent X-ray emission was detected, limiting it to $L_X/L_{\text{bol}} < 10^{-5}$. In the only previous observations of LP 944-20, an upper limit of $L_X/L_{\text{bol}} < 7 \times 10^{-5}$ was found (Neuhäuser et al. 1999). Hence, as with H α observations, the X-ray behavior of late M stars tends toward flaring activity and an absence of persistent activity at the X-ray detection limits of present instrumentation. Our work confirms this tendency.

We report here on our *Chandra* observation of an X-ray flare from the brown dwarf LP 944-20. In § 2, we describe the observation, analysis and detected flux level. In § 3, we interpret the light curve of the flare. We conclude in § 4 with a brief summary of our results and a comparison to other work.

2. CHANDRA OBSERVATION AND ANALYSIS

The observation (*Chandra* sequence number 200049) occurred on 15 Dec 1999 00:05:50–13:03:05 UTC, for 43,773 seconds. LP 944-20 was targeted at the nominal aimpoint for the ACIS-S3 chip (backside illuminated) in a faint imaging mode, with 3.2 sec time resolution. Analysis of the ACIS-S3 chip countrate during the observation showed no evidence of the background flares that sometimes appear (ACIS background calibration memo ¹), on timescales longer than 50 sec, greater than a factor of \sim few (background variability is discussed in more detail in Sec. 2.2). The standard analysis data products from *Chandra* found 117 X-ray objects in the field of view.

We now describe how we have used the observations to measure the X-ray emission from LP 944-20.

2.1. Astrometry and Source Identification

The X-ray source closest to the ACIS-S detector aimpoint was offset from the detector aimpoint by $\delta\text{RA}=-2.2''$ and $\delta\text{dec}=-8.3''$ according to the standard product astrometry. This offset is consistent with known systematic uncertainties in the *Chandra* pre-processing analysis astrometry, of the version which produced the astrometry for this observation. We performed astrometry using the absolute positions of objects in USNO-A2. We used the *Chandra* Interactive Analysis of Observations (CIAO) V1.0 software tool *celldetect* to find X-ray point source relative positions using counts detected in

PHA channels 10-400 (corresponding roughly to 0.1-4.0 keV). We found 39 X-ray sources within $10'$ of the aimpoint, with relative astrometry accurate to between 0.03-0.18". We extracted all optical source positions (from the USNO-A2 catalog) within $15''$ of the X-ray source positions. We did the same for 20 background fields for each X-ray source (a total of 780 fields), offset by increments of $15''$ from each X-ray source position, to find the USNO-A2 source density in the region of $\rho_{\text{USNO-A2}} = (5.2 \pm 0.3) \times 10^{-4}$ arcsec⁻². Of the 39 *Chandra* X-ray sources, 12 had a USNO-A2 object within $15''$. Of these 12, seven were within $1.0''$ of the offset $\delta\text{RA}=-2.2''$ and $\delta\text{dec}=-8.3''$. The probability of $n=7$ (of $m=12$) optical point sources being found within $r = 1.0''$ of a previously selected position is $P(< r) = \frac{m!}{(m-n)!n!} (1 - \exp(-\pi\rho_{\text{USNO-A2}}r^2))^n = 2 \times 10^{-17}$. Thus, the clustered USNO-A2 sources are – taken together – likely to be the optical counterparts for their corresponding X-ray sources, useful for astrometry.

To calculate the systematic shift in RA and Dec, we adopted the relative positional uncertainties for the X-ray sources found by *celldetect*, and adopted absolute positional uncertainties of $0.25''$ for USNO-A2 sources.

The astrometric correction is ($\delta\text{RA}=+2.2''$, $\delta\text{dec}=8.4''$), with an uncertainty of $\pm 0.1''$. The astrometrically corrected X-ray position of the aimpoint source is then RA=03h39m35.16s, dec=-35d25h44.0s $\pm 0.1''$ (1σ ; J2000, epoch 1999.95). The positional difference between the aimpoint source and the optical position of LP 944-20 at this epoch (Tinney 1996) is $\delta\text{RA}=-0.67 \pm 0.23''$ and $\delta\text{dec}=0.15 \pm 0.23''$, which is consistent at the 3σ level.

The likelihood of a chance alignment of a serendipitous X-ray source within $r=1''$ of an arbitrary position is $P(< r) = 0.0002$, for $\rho_{\text{X-ray}} = 7.2 \times 10^{-5}$ arcsec⁻², found from the 18 sources on the ACIS-S3 chip. We therefore identify this X-ray source with the brown dwarf LP 944-20 with 99.98% confidence on the basis of the positional coincidence.

2.2. The Flare from LP 944-20

First, we estimate the background countrate. We obtained background counts from an annulus centered on the source, with inner- and outer-radius of 4 and 140 pixels. We excluded data within 10 pixels of two X-ray sources localized by *celldetect* to be within this annulus. The total average background countrate was $(3.99 \pm 0.04) \times 10^{-6}$ counts sec⁻¹pixel⁻¹; in the limited PHA channel range of 10-400 (nominally 0.1-4.0 keV), the background countrate was $(1.0 \pm 0.02) \times 10^{-6}$ counts sec⁻¹pixel⁻¹. For nearly all the analyses we present herein, this level of background is negligible.

We extracted counts from a circle about LP 944-20 2.0 pixels in radius ($0.98''$ – the 90% enclosed energy radius at 1.5 keV, on axis). The total number of expected background counts in the source region is 2.27 ± 0.02 counts (0.1-10.0 keV), and 0.57 ± 0.01 counts (0.1-4.0 keV). We produced a (0.1-4.0 keV) light curve of 552 sec time resolution (Fig. 1). Of the 19 detected counts in the source region, 15 were detected during a 2760 sec period beginning at 1999 Dec 15 09:41:25 (UTC), which we arbitrarily define as the “flare period”. Of these, 7 were detected in a single 552 sec bin. In 80 such time bins, with an average of $19/80=0.238$ counts/bin, the probability of randomly finding 7 counts in one of 80 bins (assuming a constant countrate) is $\approx 7 \times 10^{-9}$.

The ACIS-S-BI chips suffer from short-term increases in

¹http://asc.harvard.edu/cal/Links/Acis/acis/Cal_prods/bkgmrd/11_18/bg181199.html

background countrate; these can increase the chip background countrate by up to factors of 100 across the entire chip, and in all PHA channels on timescales of seconds to minutes. The ratio of the countrates during and outside the flare period in the source region is 18-200 (3σ range, assuming Poisson statistics), while in the background region it is 0.85-1.07 (3σ , assuming Gaussian statistics). The flare cannot be from a variation in the background and must be a change in the X-ray emission of LP 944-20.

2.3. Spectral Analysis

There were 15 counts (0.1-10 keV) in the 2.0 pixel ($=0.98''$) radius about LP 944-20 during the 2760.0 seconds of the flare. We expect 0.14 background counts, which we neglect for this spectral analysis.

We performed a spectral analysis, binning the data into two bins which contained 7 and 8 counts, with a third bin of PHA channels 95-1024 which contained no counts. We fit the resulting spectrum with an assumed Raymond-Smith plasma model, implemented in XSPEC (Arnaud 1996); the best fit ($\chi^2/\nu=0.003$, for $\nu=1$ degree of freedom) found $kT=0.26_{-0.07}^{+0.1}$ keV (90% confidence), and a time-averaged flux during the 2760 seconds of $(1.5\pm 0.4)\times 10^{-14}$ erg cm^{-2} sec^{-1} ($L_X=[4.5\pm 1.2]\times 10^{25}$ erg sec^{-1} ; 0.1-10 keV), which corresponds to a flux conversion factor of 1 count = 2.8×10^{-12} erg cm^{-2} (0.1-4.0 keV) for this spectrum. This reduced chi-square value is small because the high energy bin is essentially unimportant, as there are, in the best fit model, ~ 0 counts in this bin, and thus the model can be thought of as completely determined, with only two bins and two unknowns, although the high energy bin does provide a constraint on flatter spectra, and thus on kT and flux normalization.

The uncertainty in this conversion factor depends both on the uncertainty in the Raymond-Smith spectral parameters, and on the uncertainty in the intrinsic spectrum. The best fit power-law spectrum ($\alpha_{\text{photon}}=2.6$), however, is acceptable only at 6% confidence. The best-fit black body spectrum ($kT=0.17$ keV) gives a flux 10% lower than the best-fit Raymond Smith spectrum. We estimate this as the level of spectral uncertainty in the flux conversion factor.

In Table 1, we list the L_X/L_{bol} values for the full observational period, pre-flare period, the flare period, and the peak 550 sec bin of the flare period. The uncertainties in these values are Poisson (counting statistics), plus spectral uncertainty ($\sim 10\%$). The L_X were obtained from the detected countrates, corrected for background and the Enclosed Energy fraction appropriate for our source region (0.90), and using the above flux conversion factor.

The total source fluence (including the flare) during this observation is 5.7×10^{-11} ergs cm^{-2} , corresponding to a released energy of 1.7×10^{29} ergs, and a time-averaged luminosity of $L_X=4\times 10^{24}$ erg sec^{-1} . The time-averaged L_X/L_{bol} is then 7×10^{-6} . The peak luminosity during the flare was $1.2_{-0.3}^{+0.5}\times 10^{26}$ erg sec^{-1} (including only the counting statistical uncertainty, not the 10% systematic uncertainty in the counts-energy conversion factor), corresponding to $L_X/L_{\text{bol}}\approx 2\times 10^{-4}$.

Before the flaring period, there is 1 count (0.1-4 keV) in 34535 sec, where 0.45 background counts are expected (probability $p=0.36$ – consistent with background). The 3σ upper-limit on the pre-flare flux is $<4.5\times 10^{-16}$ erg cm^{-2} sec^{-1} ($L_X < 1\times 10^{24}$ erg sec^{-1} ; $L_X/L_{\text{bol}} < 2\times 10^{-6}$). This compares to the VB 10 quiescent coronal X-ray limits from Fleming et al.

(2000) of $L_X < 1.7\times 10^{25}$ erg sec^{-1} , which is an order of magnitude greater, and $L_X/L_{\text{bol}} < 1.0\times 10^{-5}$, which is a factor of $\times 5$ greater than we find here for LP 944-20.

After the flare period, there are 3 counts in 6478 sec (0.1-4 keV) where 0.084 are expected ($p=0.0001$). Thus, there are significant counts after the flare period, which indicates that the flare event continues beyond the flaring period we defined.

3. CONSTRAINTS ON THE FORM OF THE LIGHTCURVE

Due to the low number of counts, it is difficult to measure the lightcurve parameters of this flare in a model-independent way. We therefore imposed a particular model and measured the resulting parameters. We imposed a model of an instantaneous rise/exponential decay flare, set above a constant background countrate, to compare with the 0.1-4 keV energy band data (19 counts). We assumed the background countrate from our background region. We asserted that the instantaneous rise takes place at the time of the first detected photon in the vicinity of the flare (32969 seconds into the observation). The resulting lightcurve (background+flare) must produce between 11-27 counts in total (90% confidence region of the total number of counts observed). The distribution of counts in time should match that observed over the full observation period, using a Kolmogorov-Smirnov test (Press et al. 1995), that the data and the model be consistent at the 10% level. We tested a grid of peak countrate (I_p) between 10^{-4} and 1 counts sec^{-1} , in units of 10^{-5} counts sec^{-1} , and exponential decay timescale (τ) between 1 and 2×10^4 in units of 100 sec. Based on this model and approach, we find a 90% confidence region for $\tau=5400\pm 700$ s, and $I_p=0.002-0.006$ c sec^{-1} . When we relax the constraint on start time, permitting the flare to begin at any time between 30×10^3 and 40×10^3 sec after observation start in grid units of 100 sec, the 90% confidence interval of τ is 500-7100 s, and of I_p is 0.0018-0.054 counts sec^{-1} .

This brown dwarf is known to be rapidly rotating, with a measured $V \sin i \approx 28$ km s^{-1} (Tinney & Reid 1998). For the reported bolometric luminosity of $L_{\text{Bol}} \approx (5.5\pm 0.4)\times 10^{29}$ erg sec^{-1} (Tinney 1998) and effective temperature of 2500 ± 100 K (Basri et al. 2000), the inferred radius is $R \approx (4.5\pm 0.4)\times 10^9$ cm, which is $35\pm 10\%$ smaller than the $R = 0.1R_{\odot}$ expected for an object of this mass and age (Burrows et al. 1997). The expected radius could be derived if the temperature were lowered to 2300K and the bolometric luminosity increased to 8×10^{29} erg sec^{-1} . Such changes are within the observational uncertainties. Presuming a radius of $R = 0.1R_{\odot}$, the rotation period is 4.4 hr $\sin i$. One might interpret the X-ray lightcurve as a localized flare that rotates out of view for a period and then re-appears. The implied rotation rate of ≈ 1 hour does not require an especially unlikely value of $\sin i$. However, such an interpretation is by no means required by the data to explain the variations, as these are entirely consistent with the uncertainty in the flare time evolution and Poisson counting statistics.

4. DISCUSSION AND CONCLUSIONS

We have detected an X-ray source which we identify with the brown dwarf LP 944-20, with 99.98% confidence, based on positional coincidence. The detection was during a flare, with a peak X-ray luminosity of $L_X = 1_{-0.3}^{+0.5}\times 10^{26}$ erg sec^{-1} , or $L_X/L_{\text{bol}} \approx 2\times 10^{-4}$. This flare's peak luminosity is a factor of ten below that of an X-ray flare detected from the comparably luminous M8 star VB 10 ($L_{\text{Bol}} \approx 1.7\times 10^{30}$ erg s^{-1} ; Fleming

et al. 2000). In VB 10, the peak X-ray luminosity exceeded $10^{-3}L_{\text{Bol}}$.

We have analysed the X-ray light curve with a simple sharp rise plus exponential decay model; this indicates a decay time 5400 ± 700 s when we specify the flare start-time, and in the range of 500-7100 s when we do not specify the flare start time. This implies LP 944-20 is flaring $\sim 10\%$ of the time, comparable to the amount of H α flaring among the coolest M dwarfs (Gizis et al. 2000), although the uncertainty on our value is large. The light-curve is consistent with rotational modulation, but the counting statistics are too poor to conclude that it is required, and discovery of such modulation must wait for higher signal-to-noise data. A previous attempt to detect this source in X-rays (Neuhäuser et al. 1999) placed an upper-limit on the time-averaged luminosity ($L_X < 4 \times 10^{25}$ erg s $^{-1}$) during a 66 ksec ROSAT/SPSC observation and a 220 ksec ROSAT/HRI observation. These limits are above the time-averaged luminosity we detect here ($L_X \approx 4 \times 10^{24}$ erg s $^{-1}$), and are therefore consistent with our results. X-ray variability was not discussed by these previous works; however, a cursory review of 220 ksec of ROSAT/HRI data revealed no variability on timescales of 500 sec; the detection sensitivity (5 counts in a 500 sec bin, energy conversion factor of 3.2×10^{-11} erg cm $^{-2}$ sec $^{-1}$ count $^{-1}$), is about a factor of 10 above the present peak-flare detection.

The time-averaged luminosity ($L_X=4 \times 10^{24}$ erg sec $^{-1}$) is a factor of 10^4 below the previous detections of brown dwarfs and brown dwarf candidates; the time-averaged ratio $L_X/L_{\text{bol}} (=7 \times 10^{-6})$ is factor of 10^2 below this ratio (Neuhäuser & Comerón 1998; Neuhäuser et al. 1999). This might be due to different energy production mechanisms; the previously detected brown dwarfs are young compared with LP 944-20 (~ 1 My vs. 500 My) and are still forming, while LP 944-20 is isolated and undergoing slow gravitational contraction. The persistent X-ray emission of the very young brown-dwarfs in open clusters is more analogous to the pre-main sequence T-Tauri stars – where convection is stronger, the atmospheres are less neutral, and accretion may play a role – while the flaring X-ray emission of LP 944-20 is more analogous to the flaring emis-

sion of late-type main-sequence stars, such as VB 8 and VB 10.

We estimate (order of magnitude) an eddy turnover time of ~ 1 year for LP 944-20, yielding a Rossby number of $R_0 \sim 5 \times 10^{-4}$. As discussed earlier, this is below the Rossby number limit at which the X-rays are observed to be "saturated" (at $L_X/L_{\text{bol}} \sim 10^{-3}$). That saturation level is much greater than our quiescent X-ray flux upper limit. Either the "supersaturation" suggested by Randich has strongly set in, or the connection between Rossby number and observed activity is no longer relevant. It is possible that the rapid rotation suppresses persistent coronal activity, either by forcing the magnetic field into a more organized form or by suppressing the turbulent dynamo. It is also possible that the neutrality of a cool photosphere quenches coupling between atmospheric motions and the magnetic field, which forces the field into dissipative configurations (as pointed out by Fleming et al. 2000). In any case, the detected flare requires that a magnetic field be present on LP 944-20, and that at least occasionally it is forced into a dissipative configuration high in the atmosphere.

Our results confirm the impression from previous studies of H α that stellar activity is dying at the bottom of the main sequence, at least in the form that it has in more massive late-type stars. We have pushed the limits on quiescent coronal emission levels to new lows for fully convective objects. We have also helped confirm that such objects do apparently still have magnetic fields and an ability to flare about 10% of the time.

The authors are grateful to the *Chandra* Observatory team for producing this exquisite observatory. We are grateful to Andrew Cumming for his critical reading of an early version of this paper, and to the referee Tom Fleming, for comments which dramatically improved the paper's readability. We thank Daniel Holz for encouraging us to consider the rotational modulation of the lightcurve. This research was supported by NASA Grant No. GO0-1009X and the National Science Foundation under Grant No. PHY94-07194. L. B. is a Cottrell Scholar of the Research Corporation.

REFERENCES

- Arnaud, K. A., 1996, in G. Jacoby & J. Barnes (eds.), *Astronomical Data Analysis Software and Systems V*, Vol. 101, p. 17, ASP Conf. Series
- Bailer-Jones, C. A. L. & Mundt, R., 1999, *A&A* 348, 800
- Basri, G. & Marcy, G. W., 1995, *AJ* 109, 762
- Basri, G., Mohanty, S., Allard, F., Hauschildt, P. H., Delfosse, X., Martín, E. L., Forveille, T., & Bertrand, G., 2000, *ApJ*, in press, astro-ph/0003033
- Burrows, A., Marley, M., Hubbard, W. B., Lunine, J. I., Guillot, T., Saumon, D., Freedman, R., Sudarsky, D., & Sharp, C., 1997, *ApJ* 491, 856
- Feigelson, E. D. & Montmerle, T., 1999, *ARA&A* 37, 363
- Fleming, T. A., Giampapa, M. S., & Schmitt, J. H. M. M., 2000, *ApJ* 533, 372
- Fleming, T. A., Giampapa, M. S., Schmitt, J. H. M. M., & Bookbinder, J. A., 1993, *ApJ* 410, 387
- Giampapa, M. S., Rosner, R., Kashyap, V., Fleming, T. A., Schmitt, J. H. M. M., & Bookbinder, J. A., 1996, *ApJ* 463, 707
- Gizis, J. E., Monet, D. G., Reid, N. I., Kirkpatrick, J. D., Liebert, J., & Williams, R. J., 2000, *AJ*, in press, astro-ph/0004361
- Liebert, J., Kirkpatrick, J. D., Reid, I. N., & Fisher, M. D., 1999, *ApJ* 519, 345
- Neuhäuser, R., Briceño, C., Comerón, F., Hearty, T., Martín, E. L., Schmitt, J. H. M. M., Stelzer, B., Supper, R., Voges, W., & Zinnecker, H., 1999, *A&A* 343, 883
- Neuhäuser, R. & Comerón, F., 1998, *Science* 282, 83
- Noyes, R. W., Hartmann, L. W., Baliunas, S. L., Duncan, D. K., & Vaughan, A. H., 1984, *ApJ* 279, 763
- Press, W., Flannery, B., Teukolsky, S., & Vetterling, W., 1995, *Numerical Recipes in C*, Cambridge University Press
- Randich, S., 1997, in R. A. Donahue & J. A. Bookbinder (eds.), *Cool Stars, Stellar Systems and the Sun: Tenth Cambridge Workshop*, No. 154 in *Astronomical Society of the Pacific Conference Series*, p. 501, Astronomical Society of the Pacific
- Reid, I. N., Kirkpatrick, J. D., Gizis, J. E., & Liebert, J., 1999, *ApJ* 527, L105
- Spiegel, E. A. & Zahn, J., 1992, *A&A* 265, 106
- Tinney, C. G., 1996, *MNRAS* 281, 644
- Tinney, C. G., 1998, *MNRAS* 296, L42
- Tinney, C. G. & Reid, I. N., 1998, *MNRAS* 301, 1031
- Tinney, C. G. & Tolley, A. J., 1999, *MNRAS* 304, 119
- Weiss, N. O., 1996, in M. R. E. Proctor & A. D. Gilbert (eds.), *Lectures on Solar and Planetary Dynamos*, p. 59, Cambridge University Press, Cambridge

FIG. 1.— Comparison between the 0.1-4.0 keV X-ray light curve of LP 944-20 (top panel), and the 0.1-10.0 keV background countrate (bottom panel). Crosses mark the energies (right-hand scale) of the detected counts. The vertical broken lines mark the (arbitrary) beginning and end of the flare; we refer the period prior to this as the "pre-flare" period, and after this the "post-flare" period. The variation observed in LP 944-20 is absent in the background countrate taken from a much larger area on the same chip, but away from the position of LP 944-20. This demonstrates that the variability in LP 944-20 is not due to variations in the background countrate in the chip.

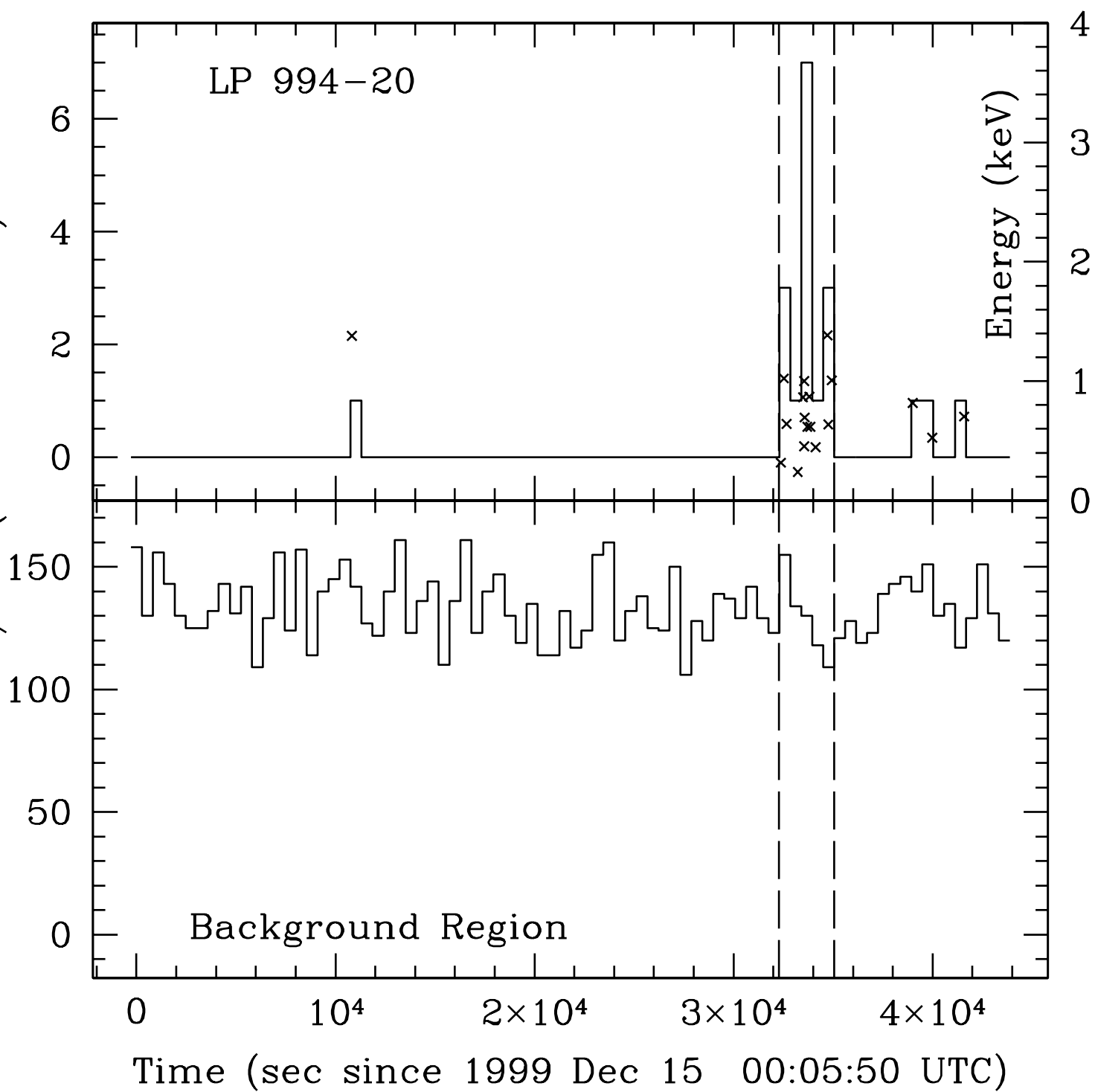


TABLE 1
 DERIVED COUNTS AND L_X/L_{bol}

Period	#Counts (bkg)	L_X/L_{bol}
Full Obs.	19 (0.57)	7×10^{-6}
Pre-flare	1 (0.44)	$< 2 \times 10^{-6}$
Flare	15 (0.14)	8×10^{-5}
Peak Flare	7 (0.02)	2×10^{-4}

NOTE.—Assumed 1 count = 2.8×10^{-12} erg cm⁻². Upper limit is 3σ .
 Source distance d=5.0 pc